Materials and methods

Data Acquisition and Preprocessing

Single-cell RNA sequencing (scRNA-seq) data from prostate cancer samples representing three clinical states were obtained from the Gene Expression Omnibus (GEO, https://www.ncbi.nlm.nih.gov/geo/) database under the accession numbers GSE274229[20], GSE137829[21], GSE141445[22], GSE181294[23], and GSE210358[24] (Table S1). The datasets comprised a total of 30 local prostate cancer samples (ADT-naïve), 32 metastatic hormone-sensitive prostate cancer (mHSPC) samples following ADT therapy, and 32 metastatic castration-resistant prostate cancer (mCRPC) samples following ADT therapy. Furthermore, spatial transcriptomics data for prostate cancer were downloaded from the GEO dataset GSE278936[25]. Additionally, bulk transcriptome datasets and corresponding clinical information for prostate cancer were sourced from The Cancer Genome Atlas (TCGA), the Chinese Prostate Cancer Genome and Epigenome Atlas (CPGEA), and the GEO datasets GSE116918[26] and GSE3325[27]. All sequencing data utilized in this study were derived from publicly available sources. We further validated the prognostic relevance of SENP6 expression using the TCGA clinical cohort.

Analysis of scRNA-seq Data

The scRNA-seq data were processed and integrated into a Seurat object using the Seurat R package (version 5.3.0)[28]. Cells were excluded if they contained fewer than 200 UMIs or more than 6,000 UMIs, expressed fewer than 200 genes, or displayed a mitochondrial gene content exceeding 20%. Potential doublets were identified and removed using the DoubletFinder R package (version 2.0.4). Datasets were integrated using Harmony (v1.2.3), and the integrated matrix was subsequently clustered following the standard Seurat workflow. We further assessed the effectiveness of Harmony-based batch correction by comparing UMAP embeddings before and after integration. The count matrix was normalized using a log-normalization approach with a scale factor of 10,000, and the top 2,000 highly variable genes (HVGs) were identified via the “vst” method in the FindVariableFeatures function. To correct for confounding effects arising from mitochondrial/ribosomal content (% UMIs), DIG signature scores, technical batch, and donor variability, the HVG matrix was z-scaled using the ScaleData function in Seurat. Dimensionality reduction was conducted in two sequential steps: principal component analysis (PCA) based on the 2,000 HVGs, followed by uniform manifold approximation and projection (UMAP) applied to the first 20 principal components using the RunUMAP function. Cell clustering was then performed by constructing a shared nearest neighbor (SNN) graph and optimizing cluster structure using the Louvain algorithm via the FindClusters function. Differentially expressed genes (DEGs) defining each subcluster were identified with FindAllMarkers, which served as the basis for subsequent tissue-specific enrichment analysis and subtype classification. Cell-cycle scores were calculated based on canonical S-phase and G2/M-phase gene sets. To minimize potential clustering bias

caused by cell-cycle heterogeneity, cell-cycle-associated variation was regressed out before dimensionality reduction and clustering. The distribution of G1, S, and G2/M phase cells was then assessed across clusters.

Cell distribution variation

The proportion of cells in each subcluster was calculated and compared across the three clinical states. To characterize the distribution patterns of each cell type among different tumor stages, scatter plots and density plots were generated to visualize cell type proportions for each patient. For identifying cell populations shared across prostate cancer states, an observed-to-expected ratio ($R_o/_e$ = observed/expected) was computed for each combination of cell cluster and cancer status[29]. Expected cell counts were derived from χ^2 contingency tables under the assumption of independence. Additionally, a correlation heatmap was used to depict expression relationships among the different cell types.

Single-cell inferred copy number alterations (CNAs)

Large-scale chromosomal alterations were inferred from scRNA-seq data using inferCNV (v1.20.0). Untreated samples served as the reference group for CNA inference in treated samples. Prior to analysis, genes with mean expression below 0.1 counts per cell were excluded. CNV signals were then denoised by applying a dynamic threshold set at 1.3 standard deviations from the mean. The resulting denoised and normalized expression matrix was organized according to genomic position. This matrix was visualized as a heatmap using the ComplexHeatmap package (v2.14.4) in R, based on 30% randomly subsampled cells from each biological group.

Cell trajectory inference

Developmental trajectories were reconstructed using CytoTRACE (v0.3.3), Monocle3 (v1.3.7), and Monocle2 (v2.32.0). Pseudotemporal ordering was performed by integrating CytoTRACE trajectory modeling with Monocle2 (v2.32.0). Highly variable genes were selected from epidermal cells using the dispersionTable function in Monocle, followed by dimensionality reduction via DDRTree. The resulting trajectory was visualized using the plot_cell_trajectory function.

Transcriptional regulatory network analysis

Transcriptional regulatory networks were reconstructed using the SCENIC pipeline (v1.1.3). Reference transcription factors (TFs) for the hg38 genome were obtained from RcisTarget, and a gene expression matrix normalized by Seurat was used as input. Co-expression modules linking transcription factors and potential target genes were first inferred using GRNBoost2. These associations were subsequently refined through cis-regulatory motif enrichment analysis performed with the ctx module, leading to the identification of regulons—defined as transcription factor and their direct target gene sets—for further analysis. To characterize subtype-specific regulatory programs in malignant tumor cells, regulon activity was quantified per cell using AUCell

enrichment scores. Differential regulon activation across subtypes was assessed with Wilcoxon rank-sum tests via the FindAllMarkers function in Seurat (parameters: min.pct = 0.2, logfc.threshold = 0.25, only.pos = TRUE). Significant regulons were visualized by hierarchical clustering based on scaled regulon activity scores.

Gene pathway enrichment analysis

Differentially expressed genes (DEGs) for each cell type were identified using the FindMarkers function in Seurat with the Wilcoxon Rank Sum test (default parameters). Genes were classified as DEGs if they met the following criteria: (1) detected in more than 25% of cells within a given cluster, and (2) exhibiting an average $\log_2$ fold change greater than 0.25 compared to other clusters. Cell type annotation was performed using a dual strategy: canonical marker genes identified through DEG analysis were cross-referenced with established literature and further validated using Seurat's FeaturePlot and VlnPlot functions. Subtype resolution for each defined cell population was achieved by reapplying Seurat's standard clustering workflow.Gene set enrichment was conducted via gene set variation analysis (GSVA) implemented in the GSVA package (v1.52.3). GO pathway analysis was performed using the R package clusterProfiler (v4.12.1). Single-cell pathway activity scoring was carried out with the AUCell R package (v1.26.0). Gene expression rankings per cell were first generated from the input expression matrix using the AUCell_buildRankings function under default settings. Canonical pathway gene sets were obtained from the Broad Institute's Molecular Signatures Database (MSigDB). For each pathway–cell pair, pathway activity was quantified as the area under the curve (AUC) score using the AUCell_calcAUC function. This score reflects the enrichment of pathway-specific genes among the top-ranking expressed genes in each cell, where an AUC value of 1.0 indicates that all pathway genes rank within the highest expression percentiles.

Spatial transcriptomics data analysis of CRPC

Spatial transcriptomics RNA-seq data were obtained from the GEO database (accession GSE278936). Data were processed using the Seurat package. Raw gene expression matrices were log-normalized with a scale factor of 10,000. Quality control filtering retained cells with 10–10,000 detected genes and 10–25,000 UMIs. The top 2,000 highly variable genes were then identified using variance-stabilizing transformation (vst). Expression values of these genes were scaled to unit variance prior to dimensionality reduction via principal component analysis (PCA). Nonlinear embeddings were generated with UMAP based on the first 30 principal components. Spatial organization patterns were visualized by projecting UMAP-derived clusters back onto the original tissue coordinates.

Spatial transcriptomics cell type deconvolution

Cell type deconvolution of the spatial transcriptomics data was performed using the RCTD algorithm within the spacexr package. Single-cell RNA sequencing data with annotated cell types were extracted, where cell type labels were converted to named

factors; nUMI vectors were also computed to construct the reference object. The spatial transcriptomics data were converted into a SpatialRNA object by extracting UMI counts from the "Spatial" assay, along with the corresponding two-dimensional tissue coordinates (x,y). The nUMI counts were then quantified for each spot. Deconvolution was executed in “full” mode—allowing multiple cell types per spot—using the create. RCTD function. The resulting cell type weight matrix was integrated into the metadata of the spatial Seurat object, while the complete deconvolution results were saved for downstream analysis of spatial cell type distributions.

Spatial Co-localization Analysis

Spatial cell–cell interactions were quantified using the mistyR package. Composition matrices obtained from RCTD deconvolution were converted into tibble format. Tissue coordinates were extracted from the corresponding Seurat object. A paraview radius was defined as the ceiling value derived from the Euclidean distance matrix. Multi-view models were trained using the run_misty pipeline

Cell culture, RNA interference and plasmid transfection

The RWPE-1 cell line was obtained from ATCC and maintained in Keratinocyte Serum-Free Medium (K-SFM; Gibco, 17005-042). Human prostate cancer cell lines—including LNCaP, C4-2, PC-3, and 22Rv1—were purchased from the Chinese Academy of Sciences Cell Bank (Shanghai, China) and cultured in standard medium supplemented with 10% fetal bovine serum (Biological Industries) and 1% penicillin/streptomycin (HyClone). All cell lines were grown at 37°C in a humidified incubator with 5% CO_2 and routinely confirmed to be free of mycoplasma contamination. siRNA transfections were performed by reverse transfection using Lipofectamine RNAiMax (Invitrogen). All siRNAs were transfected at a final concentration of 10–20 nM. The sequences of all siRNAs used in this study are provided in Table S4.

Western blotting and real-time quantitative PCR

Cells were harvested and lysed in RIPA buffer supplemented with 1% phosphatase and protease inhibitor cocktails. Protein concentration was determined using a BCA protein quantification kit (Yazyme, ZJ101). Equal amounts of protein lysates were separated by SDS-PAGE and transferred onto nitrocellulose (NC) membranes. After blocking with 5% skim milk for 1 h at room temperature, the membranes were incubated with specific primary antibodies diluted in blocking buffer overnight at 4 °C. The membranes were then washed three times (5 min per wash) with 1× TBST and incubated with HRP-conjugated secondary antibodies for 1 h at room temperature. Following another three washes with TBST, protein bands were visualized using BeyoECL Plus (BEYOTIME, P0018M).

Total RNA was extracted using TRIzol reagent (Thermo Fisher Scientific, 15596018). RNA purity and concentration were measured spectrophotometrically. Then, 500 ng of

RNA was reverse-transcribed into cDNA using the PrimeScript RT Master Mix reagent (TaKaRa, RR036A). Quantitative PCR (qPCR) was performed using the resulting cDNA, gene-specific primers (Sangon Biotech), and PowerUp SYBR Green Master Mix (Thermo, A25742). GAPDH was used as the internal reference gene. The sequences of all primers used in this study are provided in Table S4.

Tissue samples, H&E staining and immunohistochemistry staining

Human prostate cancer (PCa) and adjacent normal prostate tissue samples for SENP6 protein level analysis were obtained from the Urological Department Tissue Specimen Bank. Tissue specimens were snap-frozen in liquid nitrogen and stored at −80 °C until use.

For both hematoxylin and eosin (H&E) staining and immunohistochemistry (IHC), xenograft tumor and clinical PCa samples were fixed in formalin and embedded in paraffin. Sections of 4 μm thickness were prepared and mounted. For H&E staining, tissue sections were deparaffinized in xylene and rehydrated through a graded ethanol series (100% → 95% → 80% → 70%). The slides were then stained with hematoxylin, rinsed, and counterstained with 1% eosin. After staining, tissues were dehydrated through a reverse ethanol series, cleared in xylene, and coverslipped with mounting medium. Immunostaining was performed as previously described[30]. Anti-SENP6 antibody (sc-100585) was used to assess SENP6 expression in human prostate cancer and normal tissues. In mouse xenograft tumors, anti-SENP6 (sc-100585) and anti-Ki67 (ab15580) antibodies were applied to evaluate protein expression.

Cell Clonal proliferation assay and CCK8 cell proliferation assay

Cell proliferation was assessed using a CCK-8 kit (Beyotime, China). A total of 1,000 cells resuspended in 100 μL of medium containing 10% FBS were seeded into three replicate wells of a 96-well plate. The CCK-8 working solution was prepared by mixing 10 μL of CCK-8 reagent with 100 μL of RPMI-1640 or DMEM. Then, 110 μL of the mixture was added per well, followed by incubation for 2 h. Absorbance was measured at 450 nm.

Colony formation assay and transwell invasion assay

For the colony formation assay, subcultured cells were digested, resuspended in fresh medium, counted, and seeded into 6-cm culture dishes at a density of 1,000 cells per dish. After 14 days, the medium was removed and cells were fixed with 4% paraformaldehyde for 30 min. Following fixation, cells were stained with 0.1% crystal violet solution for 30 min, rinsed three times with pure water, and air-dried before imaging and colony counting. For the Transwell invasion assay, cell invasion ability was evaluated using Transwell chambers pre-coated with Matrigel. Cells were seeded in serum-free medium into the upper chamber, while the lower chamber contained medium with 10% FBS as a chemoattractant. After 24 h of incubation, non-invading

cells were removed from the upper chamber with a cotton swab. Cells that migrated to the lower surface were fixed, stained, and counted under a microscope.

5-Ethynyl-2'-deoxyuridine (EdU) incorporation assay

The 5-ethynyl-2′-deoxyuridine (EdU) incorporation assay was conducted using the Click-iT™ EdU Imaging Kit (Thermo Fisher, C10420) following the manufacturer's instructions. Cells were incubated with 20 μM EdU for 1 h, then fixed with 4% paraformaldehyde. After washing, cells were incubated in PBS containing 3% BSA. The Click-iT reaction cocktail was then added and incubated for 30 min. Blocking was performed using 3% BSA with 0.05% Tween-20 in PBS (PBST blocking buffer) for 1 h at room temperature. Cells were then incubated overnight at 4 °C with a primary antibody against biotin (Rabbit, Abcam, ab53494) diluted in the blocking solution.

Subcutaneous tumorigenesis experiment

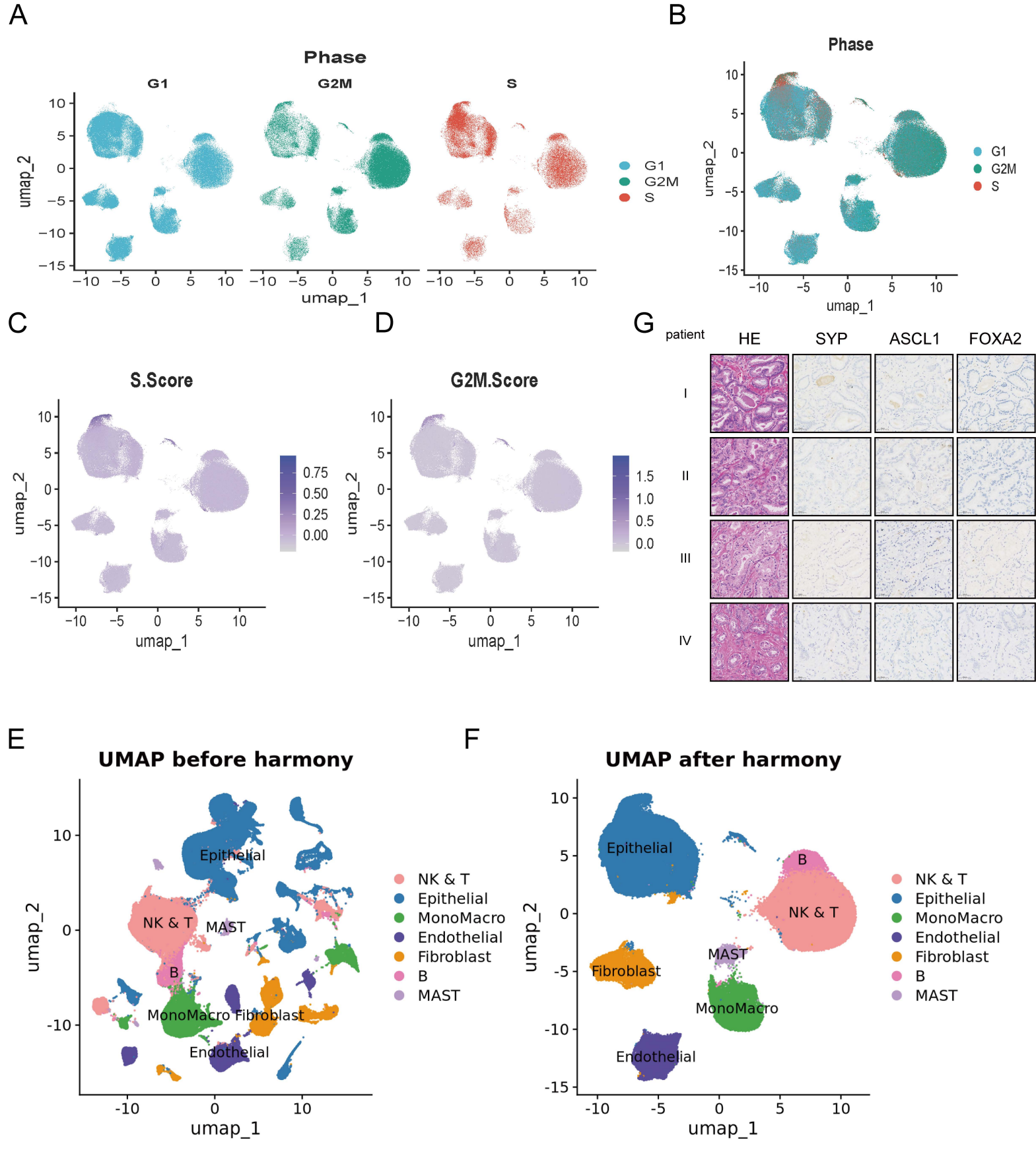
The SENP6 overexpression lentiviral vector was obtained from Youze Biotech (Changsha, Hunan). Lentivirus was produced by co-transfecting HEK293T cells with control or HA-SENP6 expression plasmids, along with the psPAX2 packaging plasmid and pMD2.G envelope plasmid, using Lipofectamine 2000. Viral supernatants were collected 48 h after transfection and stored at −80 °C for subsequent use. For in vivo studies, male NOD/SCID mice (6 weeks old, 22–24 g; Shanghai SLAC Laboratory Animal Co., Ltd.) were housed under specific pathogen-free conditions in the animal center of Hospital, with temperature maintained at 22 ± 0.5 °C, humidity at 60% ± 3%, and an automated 12 h light/dark cycle. Food and water were provided ad libitum. Mice were divided into experimental groups and injected subcutaneously on the right flank with a 1:1 mixture of cells and Matrigel. Tumor size was measured every other day using a caliper for 6 weeks post-injection. At the endpoint, mice were euthanized, and tumors were excised and processed for further analysis.

Colocalization of immunofluorescence staining

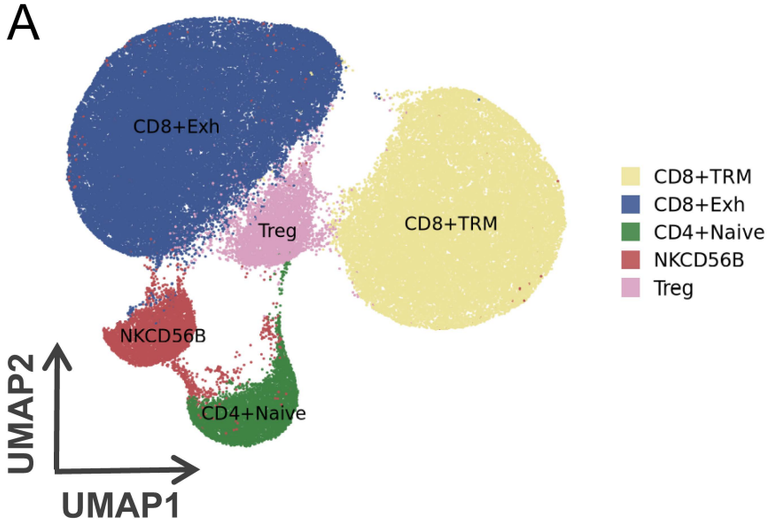
Cells on glass coverslips were washed twice in PBS and fixed with 4% paraformaldehyde (PFA) for 18mins. Cells were permeabilized with 0.5% (v/v) Triton X-100 for 7mins and incubated with fresh blocking solution (PBS containing 0.05%Tween-20 and 3%BSA) for 1h. Primary antibodies were diluted 1:1000 in blocking solution and added to cells for overnight refrigerated. Next, cells were washed three times with PBST(PBS containing 0.05%Tween-20) for 5mins and incubated with Alexa-coupled secondary antibodies (488nm, 555nm, 647nm; diluted 1:1,000 in blocking solution) for 1 h at RT. Then, cells were washed three times with PBST and mounted on slides with Prolong Gold Anti-fade reagent with DAPI (Life Technologies). Once the Prolong Anti-fade polymerized and cured, cells were visualized by conventional fluorescence with 10X and 60X Plan I objective (1.4 oil) using a Nikon Eclipse Ni.

Molecular Docking and Interaction Domain Analysis

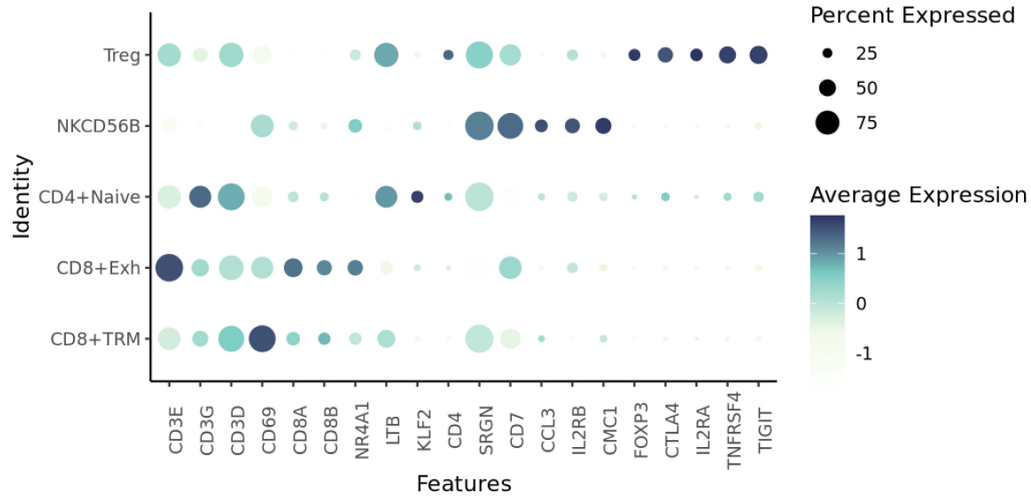
The amino acid sequences of SENP6 and AR were obtained from the UniProt database. Protein domain information and related functional annotations were retrieved from the UniProt and InterPro databases. Protein–protein interaction between SENP6 and AR was modeled using AlphaFold 3. The amino acid sequences of SENP6 and AR were used as input to predict the three-dimensional structure of the SENP6–AR complex. The predicted structure was subsequently subjected to standardized processing in PyMOL, including removal of water molecules, addition of hydrogen atoms, and structural optimization, followed by energy minimization to reduce potential steric clashes and optimize the protein conformation. The resulting complex structure was used to analyze the potential binding mode and interaction interface between SENP6 and AR. Protein domain information obtained from UniProt and InterPro was further integrated to assess the potential regions involved in the SENP6–AR interaction.


A
Phase
G1
G2M
S
umap_2
umap_1
B
Phase
C
S.Score
D
G2M.Score
G
patient
HE
SYP
ASCL1
FOXA2
I
II
III
IV
E
UMAP before harmony
Epithelial
NK & T
MAST
B
MonoMacro
Fibroblast
Endothelial
F
UMAP after harmony

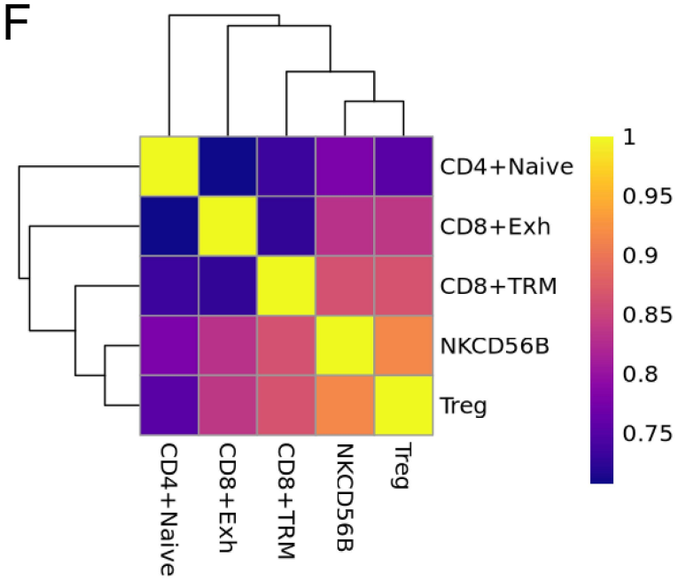
A


CD8+Exh
Treg
CD8+TRM
NKCD56B
CD4+Naive
UMAP2
UMAP1
CD8+TRM
CD8+Exh
CD4+Naive
NKCD56B
Treg

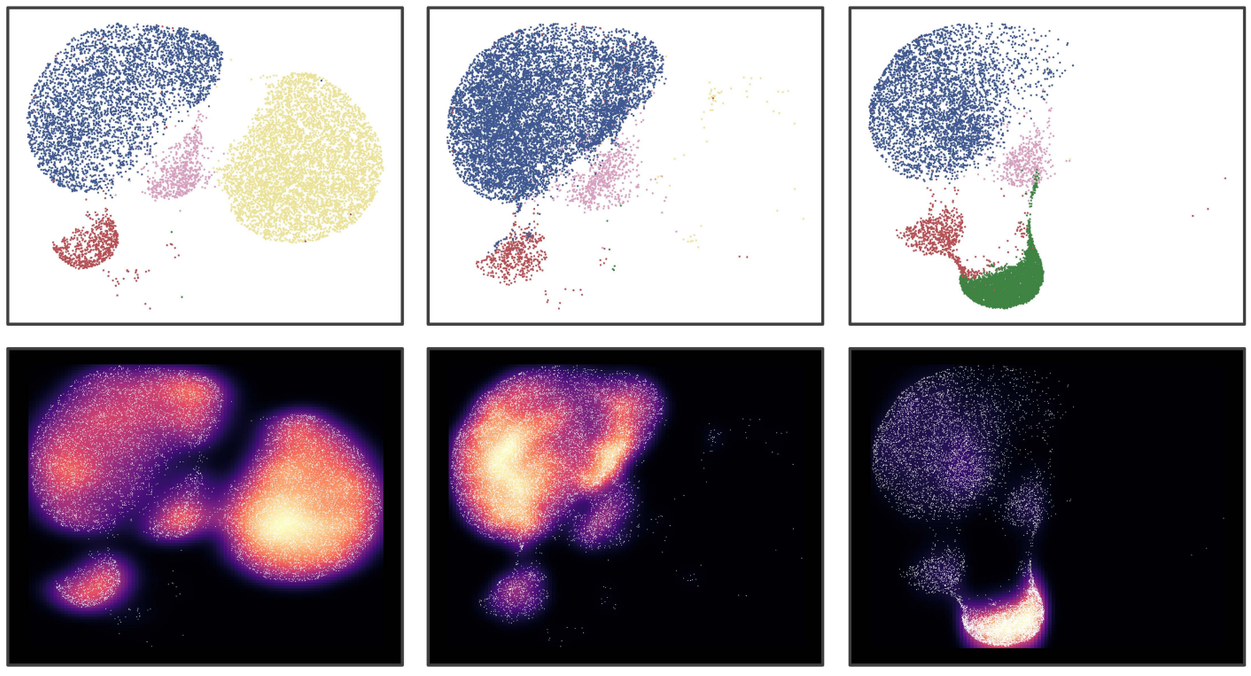
B


Treg
NKCD56B
CD4+Naive
CD8+Exh
CD8+TRM
Identity
CD3E
CD3G
CD3D
CD69
CD8A
CD8B
NR4A1
LTB
KLF2
CD4
SRGN
CD7
CCL3
IL2RB
CMC1
FOXP3
CTLA4
IL2RA
TNFRSF4
TIGIT
Features
Percent Expressed
25
50
75
Average Expression
1
0
-1

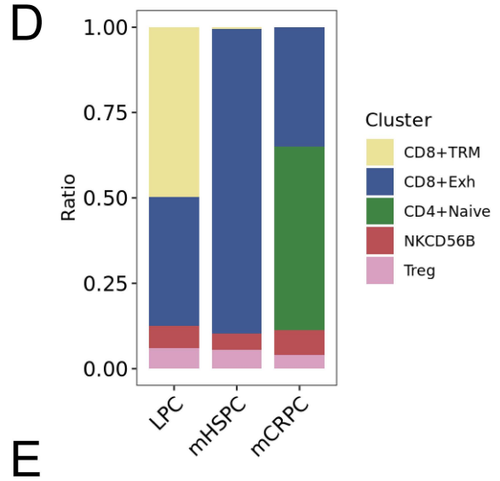
F


CD4+Naive
CD8+Exh
CD8+TRM
NKCD56B
Treg
1
0.95
0.9
0.85
0.8
0.75

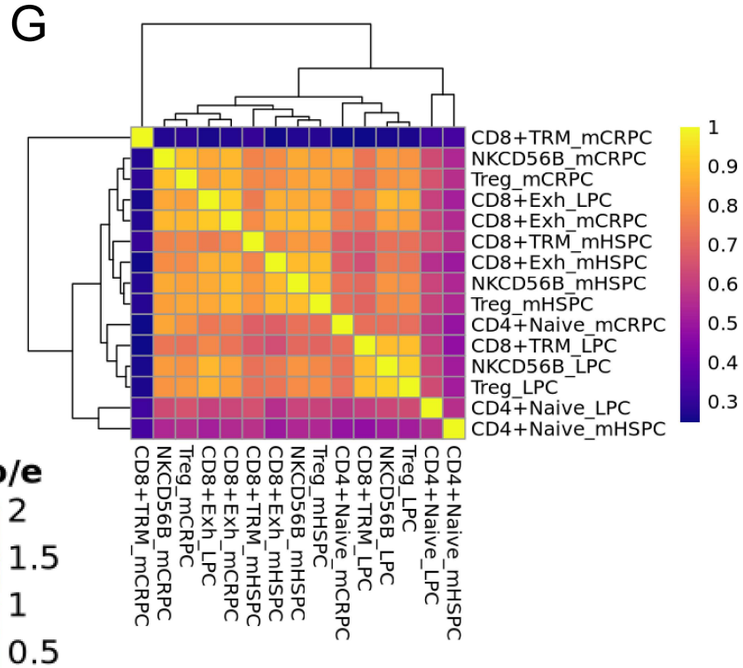
C


LPC
mHSPC
mCRPC

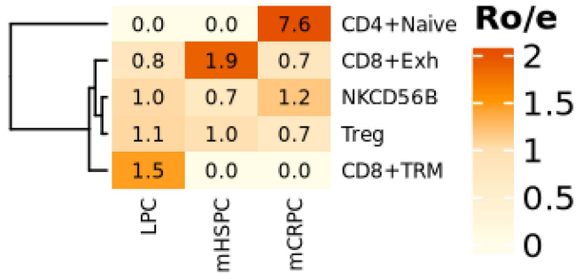
D


1.00
0.75
0.50
0.25
0.00
Ratio
LPC
mHSPC
mCRPC
Cluster
CD8+TRM
CD8+Exh
CD4+Naive
NKCD56B
Treg

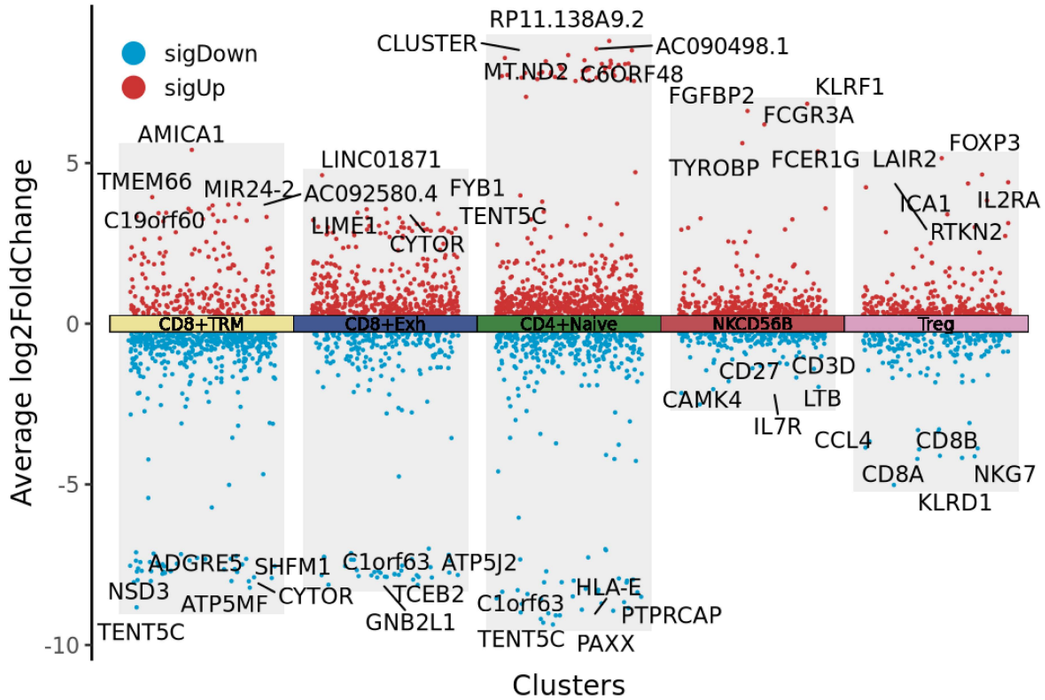
G

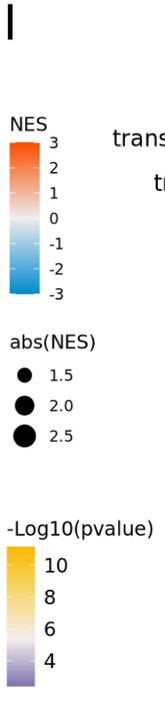

CD8+TRM_mCRPC
NKCD56B_mCRPC
Treg_mCRPC
CD8+Exh_LPC
CD8+Exh_mCRPC
CD8+TRM_mHSPC
CD8+Exh_mHSPC
NKCD56B_mHSPC
Treg_mHSPC
CD4+Naive_mCRPC
CD8+TRM_LPC
NKCD56B_LPC
Treg_LPC
CD4+Naive_LPC
CD4+Naive_mHSPC
1
0.9
0.8
0.7
0.6
0.5
0.4
0.3

E

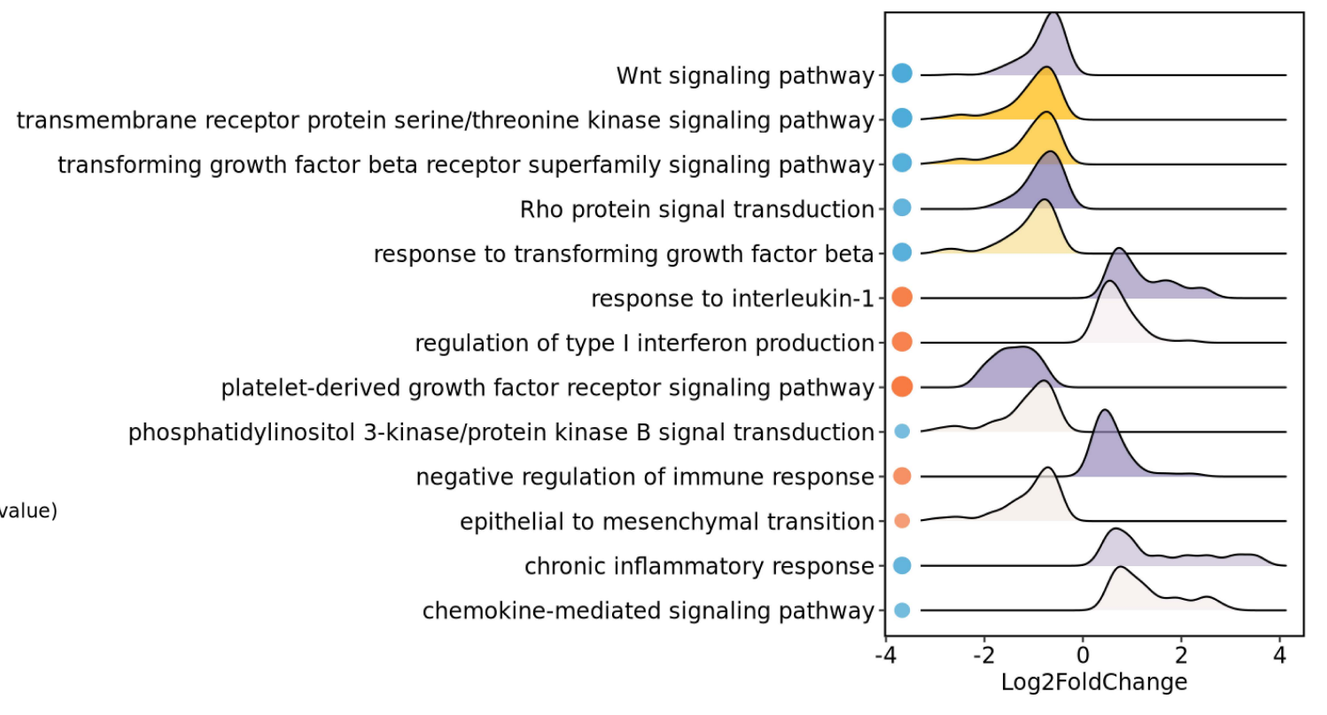

0.0 0.0 7.6 CD4+Naive
0.8 1.9 0.7 CD8+Exh
1.0 0.7 1.2 NKCD56B
1.1 1.0 0.7 Treg
1.5 0.0 0.0 CD8+TRM
LPC
mHSPC
mCRPC
Ro/e
2
1.5
1
0.5
0

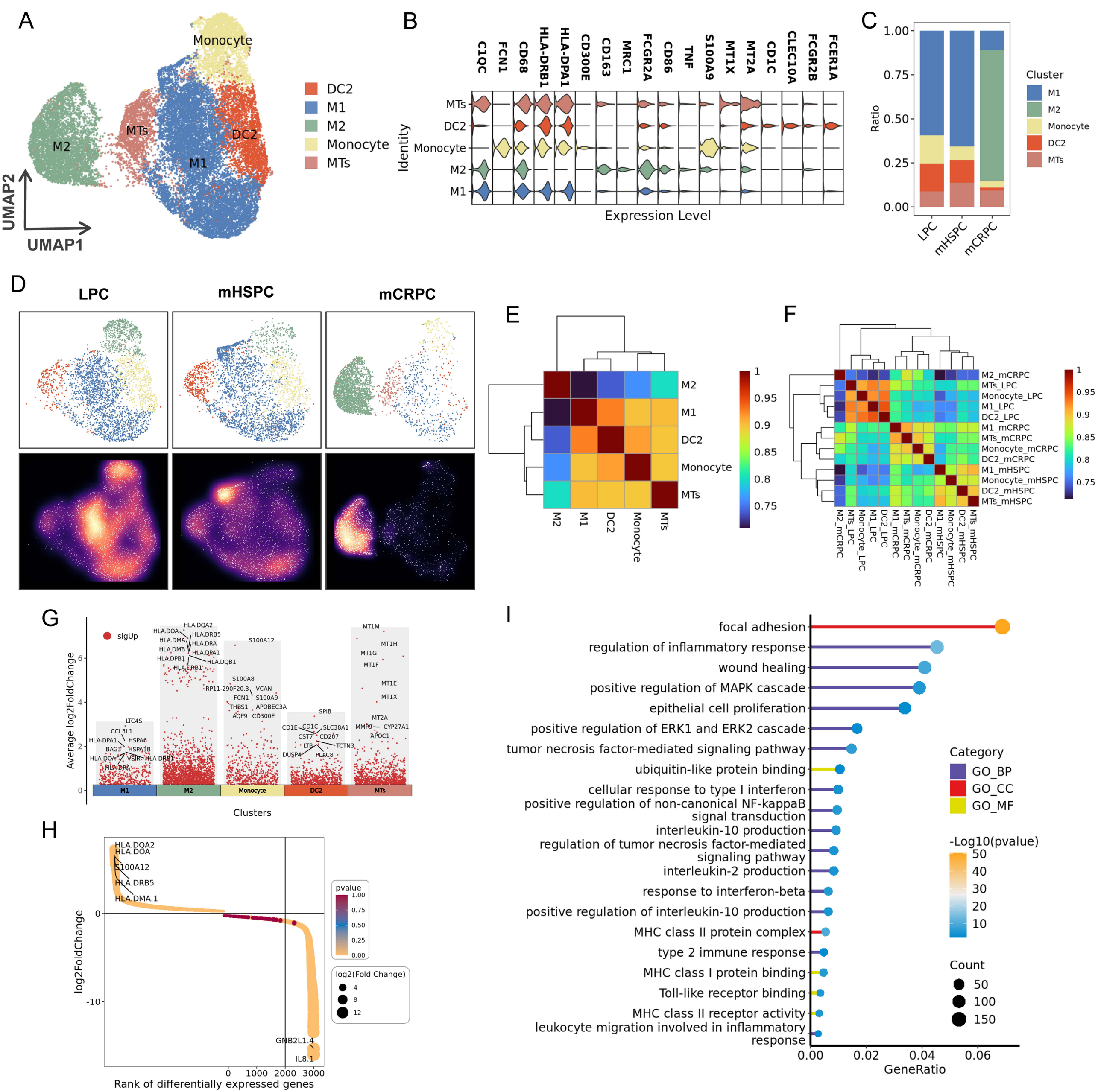
H

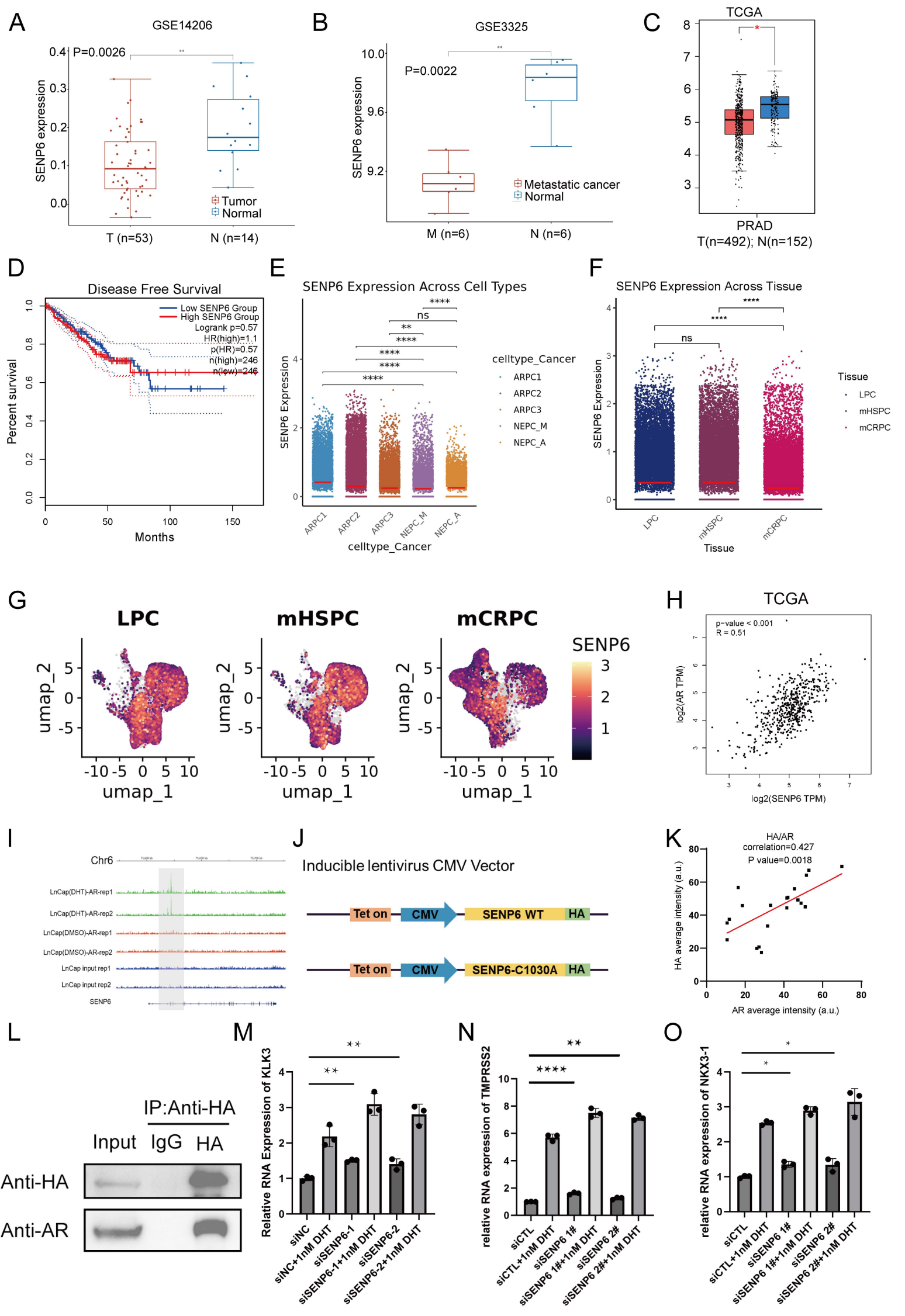

sigDown
sigUp
Average log2FoldChange
5
0
-5
-10
CD8+TRM
CD8+Exh
CD4+Naive
NKCD56B
Treg
RP11.138A9.2
CLUSTER
AC090498.1
MT.ND2
C6ORF48
FGFBP2
KLRF1
FCGR3A
AMICA1
LINC01871
TYROBP
FCER1G
LAIR2
FOXP3
TMEM66
MIR24-2
AC092580.4
FYB1
ICA1
IL2RA
C19orf60
LIME1
CYTOR
TENT5C
RTKN2
CD27
CD3D
CAMK4
LTB
IL7R
CCL4
CD8B
CD8A
NKG7
KLRD1
ADGRE5
SHFM1
C1orf63
ATP5J2
NSD3
ATP5MF
CYTOR
TCEB2
C1orf63
HLA-E
PTPRCAP
GNB2L1
TENT5C
PAXX
TENT5C
Clusters

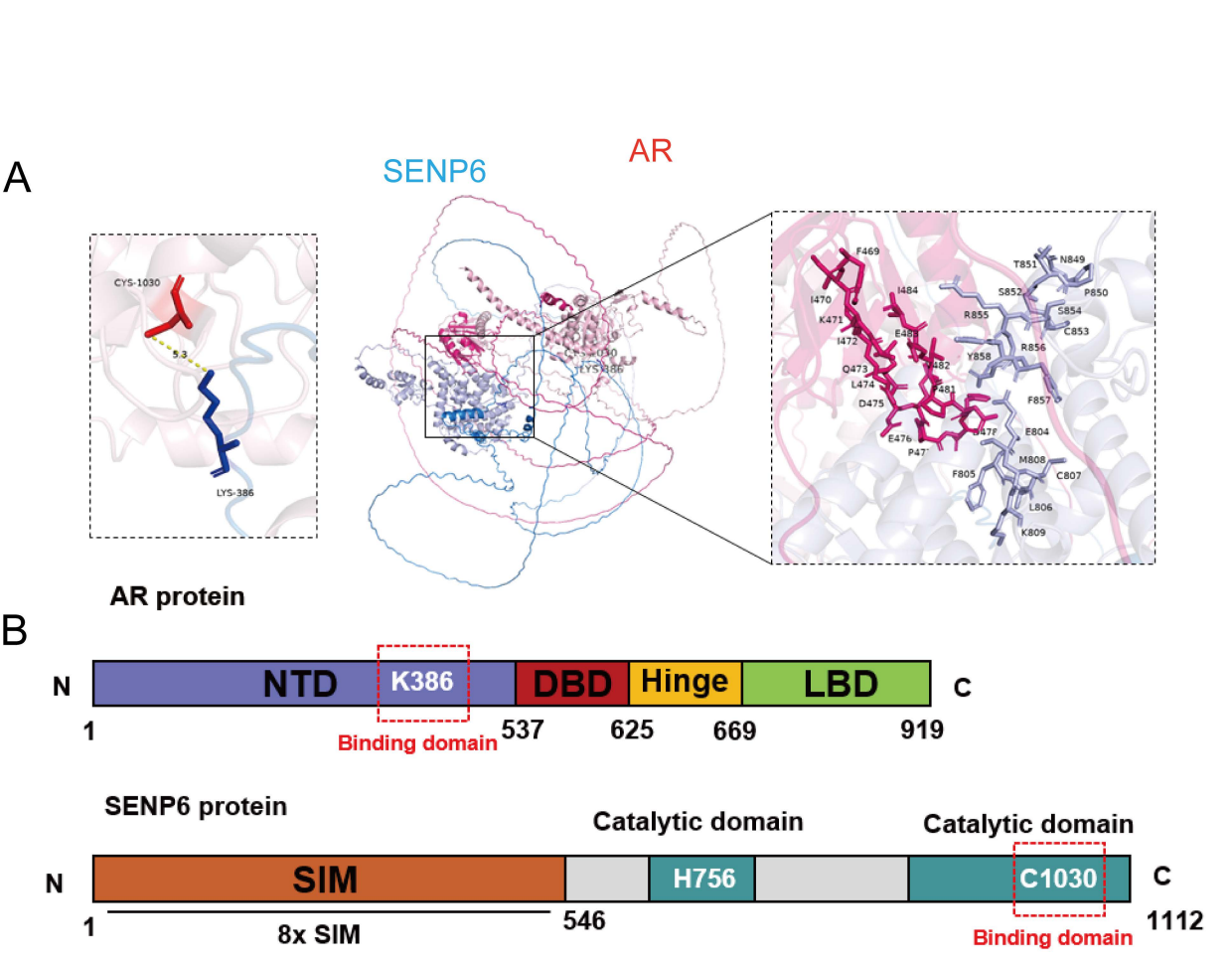

NES
3
2
1
0
-1
-2
-3
abs(NES)
1.5
2.0
2.5
-Log10(pvalue)
10
8
6
4

I


Wnt signaling pathway
transmembrane receptor protein serine/threonine kinase signaling pathway
transforming growth factor beta receptor superfamily signaling pathway
Rho protein signal transduction
response to transforming growth factor beta
response to interleukin-1
regulation of type I interferon production
platelet-derived growth factor receptor signaling pathway
phosphatidylinositol 3-kinase/protein kinase B signal transduction
negative regulation of immune response
epithelial to mesenchymal transition
chronic inflammatory response
chemokine-mediated signaling pathway
-4
-2
0
2
4
Log2FoldChange


A
Monocyte
M2
MTs
M1
DC2
UMAP2
UMAP1
DC2
M1
M2
Monocyte
MTs
B
C1QC
FCN1
CD68
HLA-DRB1
HLA-DPA1
CD300E
CD163
MRC1
FCGR2A
CD86
TNF
S100A9
MT1X
MT2A
CD1C
CLEC10A
FCGR2B
FCER1A
MTs
DC2
Monocyte
M2
M1
Identity
Expression Level
C
1.00
0.75
0.50
0.25
0.00
Ratio
LPC
mHSPC
mCRPC
Cluster
M1
M2
Monocyte
DC2
MTs
D
LPC
mHSPC
mCRPC
E
M2
M1
DC2
Monocyte
MTs
1
0.95
0.9
0.85
0.8
0.75
F
M2_mCRPC
MTs_LPC
Monocyte_LPC
M1_LPC
DC2_LPC
M1_mCRPC
MTs_mCRPC
Monocyte_mCRPC
DC2_mCRPC
M1_mHSPC
Monocyte_mHSPC
DC2_mHSPC
MTs_mHSPC
1
0.95
0.9
0.85
0.8
0.75
G
sigUp
Average log2FoldChange
Clusters
M1
M2
Monocyte
DC2
MTs
HLA.DQA2
HLA.DOA
HLA.DRB5
HLA.DMA
HLA.DRA
HLA.DMB
HLA.DPA1
HLA.DPB1
HLA.DQB1
HLA.DRB1
S100A12
S100A8
RP11-290F20.3
VCAN
FCN1
S100A9
THBS1
APOBEC3A
AQP9
CD300E
SPIB
CD1E
CD1C
SLC38A1
CST7
CD207
LTB
TCTN3
DUSP4
PLAC8
MT1M
MT1H
MT1G
MT1F
MT1E
MT1X
MT2A
MMP9
CYP27A1
APOC1
LTC4S
CCL3L1
HLA-DPA1
HSPA6
BAG3
HSPA1B
HLA-DOA
VSIR
HLA-DRB1
HLA-DRA
H
HLA.DQA2
HLA.DOA
S100A12
HLA.DRB5
HLA.DMA.1
GNB2L1.4
IL8.1
log2FoldChange
Rank of differentially expressed genes
pvalue
1.00
0.75
0.50
0.25
0.00
log2(Fold Change)
4
8
12
I
focal adhesion
regulation of inflammatory response
wound healing
positive regulation of MAPK cascade
epithelial cell proliferation
positive regulation of ERK1 and ERK2 cascade
tumor necrosis factor-mediated signaling pathway
ubiquitin-like protein binding
cellular response to type I interferon
positive regulation of non-canonical NF-kappaB signal transduction
interleukin-10 production
regulation of tumor necrosis factor-mediated signaling pathway
interleukin-2 production
response to interferon-beta
positive regulation of interleukin-10 production
MHC class II protein complex
type 2 immune response
MHC class I protein binding
Toll-like receptor binding
MHC class II receptor activity
leukocyte migration involved in inflammatory response
Category
GO_BP
GO_CC
GO_MF
-Log10(pvalue)
50
40
30
20
10
Count
50
100
150
0.00
0.02
0.04
0.06
GeneRatio


A
GSE14206
P=0.0026
SENP6 expression
Tumor
Normal
T (n=53)
N (n=14)
B
GSE3325
P=0.0022
SENP6 expression
Metastatic cancer
Normal
M (n=6)
N (n=6)
C
TCGA
PRAD
T(n=492); N(n=152)
D
Disease Free Survival
Low SENP6 Group
High SENP6 Group
Logrank p=0.57
HR(high)=1.1
p(HR)=0.57
n(high)=246
n(low)=246
Percent survival
Months
E
SENP6 Expression Across Cell Types
SENP6 Expression
celltype_Cancer
ARPC1
ARPC2
ARPC3
NEPC_M
NEPC_A
F
SENP6 Expression Across Tissue
SENP6 Expression
Tissue
LPC
mHSPC
mCRPC
G
LPC
mHSPC
mCRPC
umap_1
umap_2
SENP6
H
TCGA
p-value < 0.001
R = 0.51
log2(AR TPM)
log2(SENP6 TPM)
I
Chr6
LnCap(DHT)-AR-rep1
LnCap(DHT)-AR-rep2
LnCap(DMSO)-AR-rep1
LnCap(DMSO)-AR-rep2
LnCap input rep1
LnCap input rep2
SENP6
J
Inducible lentivirus CMV Vector
Tet on
CMV
SENP6 WT
HA
Tet on
CMV
SENP6-C1030A
HA
K
HA/AR
correlation=0.427
P value=0.0018
HA average intensity (a.u.)
AR average intensity (a.u.)
L
IP:Anti-HA
Input
IgG
HA
Anti-HA
Anti-AR
M
Relative RNA Expression of KLK3
siNC
siNC+1nM DHT
siSENP6-1
siSENP6-1+1nM DHT
siSENP6-2
siSENP6-2+1nM DHT
N
relative RNA expression of TMPRSS2
siCTL
siCTL+1nM DHT
siSENP6 1#
siSENP6 1#+1nM DHT
siSENP6 2#
siSENP6 2#+1nM DHT
O
relative RNA expression of NKX3-1
siCTL
siCTL+1nM DHT
siSENP6 1#
siSENP6 1#+1nM DHT
siSENP6 2#
siSENP6 2#+1nM DHT


A
SENP6
AR
CYS-1030
5.3
LYS-386
F469
I470
K471
I472
I484
E485
Q473
L474
D475
E476
P477
Y482
F481
T851
N849
S852
P850
R855
S854
C853
R856
Y858
F857
E804
M808
C807
F805
L806
K809
AR protein
B
N
NTD
K386
DBD
Hinge
LBD
C
1
Binding domain
537
625
669
919
SENP6 protein
Catalytic domain
Catalytic domain
N
SIM
H756
C1030
C
1
8x SIM
546
Binding domain
1112